Nanochem Res 8(1): 50-56, Winter 2023

RESEARCH PAPER

Determination of volatile compounds from Satureja hortensis L with a Metal-organic framework on copper nanoarrays

Marzieh Piryaei

Department of Chemistry, Faculty of Science, University of Maragheh, Maragheh, Iran

ARTICLE INFO

Article History:
Received 04 Oct 2022
Accepted 23 Jan 2023
Published 21 Jan 2023

Keywords:
Essential oil
Metal–organic frameworks
Microextraction (MOFs)
Satureja hortensis L

ABSTRACT

Metal-organic frameworks as porous materials are highly advantageous over other porous carriers like mesoporous silica or zeolites. They provide advantages for biomolecule release and their adsorption characteristics offer many opportunities. Thus, they present high applicability in medicine and biology. Metal-organic frameworks (MOF) possess appealing structures and usages including high surface area, homogenous structured nanoscale cavities, and excellent thermal stability. Therefore, they can be a new sorbent alternative for preparing samples. In the present study, a MOF fiber application for solid-phase microextraction is reported. The MOF fiber is in nano size and has a high surface area. 3D and oriented organizations of MOF materials are vital so that they may be utilized as the fiber coating for microextraction in solid-phase for volatile substances in the medicinal herbs. In order to make Cu-based MOFs into three-dimensional hierarchical nanoarray structures, a coordination replication approach is created. To this end, $Cu(OH)_2$ nanorod arrays are used as a sacrificial template. $Cu(OH)_2$ nanorod arrays serving as Cu origin provided coordination with organic ligands for forming MOF crystals and 3D substrate for supporting Cu-based MOF growth. Following the presentation of the fiber, essential oils of Satureja hortensis L were determined using GC-MS. Ease of use, shorter analysis period, inexpensive tools as well as a high rate of recovery are advantages of the proposed approach compared to ordinary analysis approaches.

How to cite this article
Piryaei M., Determination of volatile compounds from Satureja hortensis L with a Metal-organic framework on copper nanoarrays. Nanochem Res, 2023; 8(1): 50-56. DOI: 10.22036/ncr.2023.01.005

INTRODUCTION

Due to remarkable adsorption characteristics and associated applications of MOFs like gas storage, sensing, separation, drug transfer, and catalysis, they have recently drawn considerable attention [1]. Self-assemblage between organic ligands and metal ion forms MOFs. These frameworks are considered polymers due to their infinite coordination-bonded structures. They consist of metal ions which function as connectors or nodes and make bridges to ligands functioning as linkers [2]. The efficiency of MOFs for analytical chemistry is high owing to their exceptional characteristics, including homogenous structured nano-scale cavities, high adsorption affinity, large surface area, suitable thermal stability, pore topology, distinctive structures, and usage in pore functionality, and outer-surface modification [3]. In addition, these frameworks have open metal sites, which notably allow improved molecule adsorption with varying polarity [4, 5].

* Corresponding Author Email: *m.piriyaei@gmail.com*

The tailored nanoporous strong MOFs, in contrast to the more common microporous inorganic materials like zeolites, are made by self-assembly and have a very large surface area (over 5000 m^2 g^{-1}). They use metal ions as coordination centers and are linked together by a variety of rigid-rod-like organic bridging ligands. Through this structure, MOFs are given open metal sites within the skeleton, organic functioning, great mechanical and thermal stability, and customizable options. MOFs are used successfully in energy conversion and gas capture due to their ultrahigh porosity, crystalline nature, controlled pore size, and highly structured structures.

Due to the synergistic effects between the functional units, it is also possible to create improved composites by rationally mixing MOFs with other functional substances. These composites will outperform their individual components. Further, a variety of nanostructured MOFs have been investigated as precursors for the synthesis of various nanomaterials, ranging from carbon-based materials to metal-based compounds (such as oxides, carbides, phosphides, and chalcogenides) with regular porous architectures. The significant advantages of MOF-based compounds in component adjustment and structural enhancement are reflected in the development of MOFs derivatives [6-11].

Solid-phase microextraction (SPME) is a sampling method and is regarded as a preconcentration approach, with such features as a quick diffusion rate, solvent-free and high enrichment factor. SPME was originally presented for analyzing volatile substances at trace levels. Particularly, headspace solid-phase microextraction (HS-SPME) is directly in relationship with the analytes, and has a large enrichment factor. Thus, it is regarded as a sampling method appropriate for volatile substances. It has been reported that the extraction performance is determined by the nature of SPME coatings [12,13].

Hence, the focus of most recent studies on SPME has been on preparing and characterizing novel sorbents with improved selectivity and sensitivity for specified analytes, as well as notable mechanical and chemical stability. MOF coating applicability was evaluated in the present study. For this purpose, an SPME device made in the laboratory and GC–MS were used to extract and determine volatile substances from medicinal herbs.

EXPERIMENTAL

Reagents and materials

All solvents and terephthalic acid used in this study were obtained from the Fluka (Buchs, Switzerland, www. sigmaaldrich.com) or Merck (Darmstadt, Germany, www. merck.de) companies. The aerial parts of *Satureja hortensis* L were harvested in July 2019 near the city of Maragheh, in the northwest of Iran. The plant materials were dried in the air and stored in sealed bags in a cool place.

Hydrodistillation (HD) apparatus and procedure

Air-dried aerial sections of *Satureja hortensis* L (100 g) were powdered. Then, a Clevenger-type device was used for hydrodistillation for two hours. In short, the herb was plunged into water, and it was then warmed up to the boiling point. At this stage, the essential oil vapor and water vapor were provided for which a condenser was used to collecting them. The distillate isolation and drying were done over anhydrous sodium sulfate. The storage temperature for the resulting oil was 4 °C, and it was ten analyzed by GC-MS. Based on the sample dry weight of 0.28% (w/w), the yield of yellow oil was obtained from aerial sections of *Satureja hortensis* L.

Apparatus

For determination, a Hewlett-Packard Agilent 7890A series GC and an Agilent 5975C mass-selective detector system, and a split/splitless injector were employed. MS operation mode was EI (70 eV). Helium (99.999 %) served as a carrier gas with a flow-rate of 1 mL min^{-1}. A 30 m×0.25 mm HP-5 MS column was used for separation. The column film thickness was 0.25 μm. The temperature in the column was 50 °C which was raised to 180 °C at the rate of 15 °C min^{-1}. It later was increased to 260 °C at the rate of 20 °C min^{-1}, and the temperature stayed at this degree for five minutes. The temperature of the injector was 260 °C, and injection operations were all performed on the splitless state for two minutes. The ion source temperature, GC–MS interface temperature, and quadrupole temperature were 230, 280, and 150 °C. Wiley 7 N Mass Spectral Library was used for identifying compounds. Acquisition and quantification of mass spectra for the compounds were conducted in the selected ion monitoring (SIM) mode. A Seron AIS-2100 SEM was utilized for the observation of the morphological structure

of developed nanocomposites. A domestic SPME tool was employed to hold and inject the prepared fiber into the GC–MS injection port. The fiber conditioning in the injection port of a GC was carried out for one hour. The identification of volatile oil components was performed by calculating retention indexes of the components under temperature-programmed circumstances for n-alkanes (C6–C24) and the oil on an HP-5MS column under identical circumstances. To identify compounds individually, the mass spectra of compounds were compared with the internal reference mass spectra library or with original compounds and approved by comparing their retention indexes with original compounds or with the values given in previous studies. The library was made by the use of pure substances or with original compounds and approved by comparing their retention indexes. Gas chromatograms were used for obtaining Kovats' retention indexes of the components. For this purpose, interpolation between bracketing *n*-alkanes was done.

Cu wire anodization method

$Cu(OH)_2$ nano-rod arrays were synthesized on commercial cu wires using a modified anodization approach presented by Xu et al. [14]. Detergent solution was used for degreasing and cleaning Cu-wires (with a length of 10 cm, 200 mμ O.D.). For the removal of organic contaminating materials and oxide layer, they were diluted by HCl solution in ambient temperature using an ultrasonic bath for one minute. Afterward, they were washed with methanol and deionized water, and then an oven was used for drying them at 50 ºC. Then, $Cu(OH)_2$ nanotube arrays were synthesized on Cu substrate through direct copper anodization in 3.0 M KOH solution. A constant current approach at a constant current density (3mA cm^{-2}) was employed for 25 minutes in a three-electrode system. In this system, an SCE and a platinum electrode served as the reference electrode and auxiliary electrode. Afterward, anodized wires were removed from the solution. Finally, the wires were cleansed using distilled water and dried.

Synthesis of hierarchical MOF on Cu nanoarrays

Xu et al. presented an anodization technique for synthesizing $Cu(OH)_2$ nanorod arrays[14]. A simple solvothermal path helps MOF formation on $Cu(OH)_2$ nanorod template. Typically, 20 mmol of terephthalic acid (H_2BDC) is diffused in benzyl alcohol (16 mL) in a Teflon stainless-steel autoclave. Then, $Cu(OH)_2$ nanorod arrays on 5 cm Cu wire are put in the solution. The autoclave is placed in the oven in 100 °C temperature for 20 hours after sonication. Afterward, the autoclave was cooled naturally to ambient temperature. At the end, the blue film was rinsed with fresh methanol, and it was dried for three hours at 60 °C. For cleaning and conditioning the developed SPME fiber, it was placed into a GC injection port at 260 °C for one hour in a helium medium.

The headspace MOF solid phase microextraction (MOF-HS-SPME) procedure

SPME was conducted with synthesized nanocomposite fiber, which was mounted on its SPME apparatus. A thermo-stated water bath was utilized for controlling extraction temperature. The retained compounds on fiber were thermally desorbed at 260 °C while keeping close the injector's split valve on the GC at varying time periods. The powdered plant (3 g) was delivered into a round bottom flask (25 mL) placing on a magnetic stirrer. The SPME probe having analytes from the sample was taken out of the vial when extraction time was reached. For thermal desorption, it was then inserted into the GC injection port.

RESULTS AND DISCUTION

MOFs as the porous materials are highly advantageous over other porous carriers like mesoporous silica or zeolites. They provide advantages for biomolecule release and their adsorption offer many opportunities. Thus, they present high applicability in medicine and biology. In the present study, MOF application for extracting essential oils from *Satureja hortensis* was investigated. SPME fiber was used for examining the impacts of various factors, including the temperature of extraction, extraction time, and sample weight on the amount of volatile oils extracted from the herb.

Temperature impact

Fig. 1 indicates the results for different extraction temperatures (50-100◦C), where the extraction temperature impact on the total peaks of the resulting compounds and individual peaks of the four substances extracted from *Satureja hortensis* is indicated. The extraction temperature significantly affects the extraction as it influences the distribution coefficients of substances between

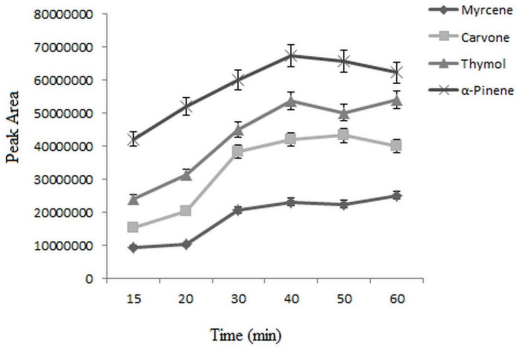

Fig. 1. Effect of extraction time on extraction efficiency

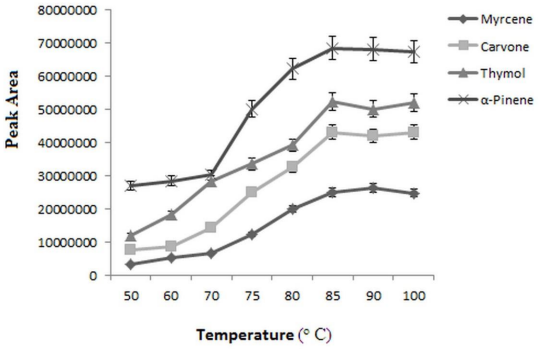

Fig. 2. Effect of extraction temperature on extraction efficiency.

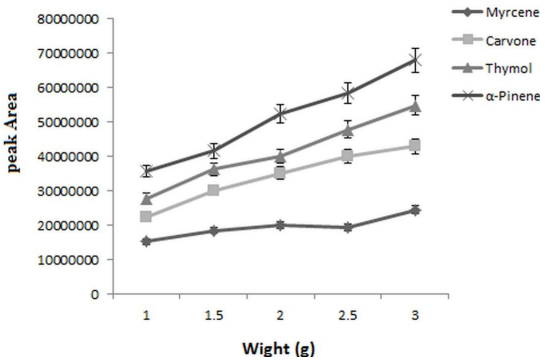

Fig. 3. Effect of sample weight on extraction efficiency.

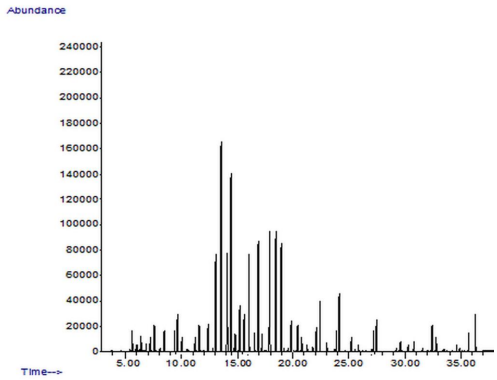

Fig 4: GC chromatogram for volatile oils

headspace and sample and between fiber and headspace. As observed, the total peaks and the individual peaks showed an increase with the rise in temperature up to 85◦ C for fiber.

Extraction time impact

Fig. 2 indicates the variation in the extraction time between 15 to 60 minutes. It shows the same trend between individual peaks and the total peaks of the target substances, implying the tendency of peaks with extraction time. The individual peaks profile, as well as the total peaks profile, demonstrate that the highest peak was obtained at 40 minutes. Longer extraction times did not show any impact on the extraction efficiency.

Sample mass

There is generally an increase in analyte signals by the rise in the amount of sample. However, it should be noted that a very large amount of sample influences the efficiency of extraction. Furthermore, the larger sample amount does not mean better outcomes. In this paper, the range of the sample amount was 1.0-3.0 g. Fig. 3 indicates the impact of sample amount on the individual and total peaks related to four compounds. With increasing the sample amount to 3 g, a rise was also observed in the individual and total peaks. In the case that the sample amount meets the sensitivity condition, it can be an appropriate criterion for analysis. A large sample amount could sometimes make a problem in sampling in a MOF-SPME procedure. Its reason is the static adsorption of sample powder to the fiber, particularly in cases of using a fine-powdered sample for an assay.

Added water

Because of this structure, water vapor (humidity) could be influenced by the ability of the fiber for adsorbing volatile substances of *Satureja hortensis*. Thus, varying amounts of water was added to samples under optimal circumstance so that the humidity impact can be examined, the results of which are illustrated in Fig. 4. In other words, the water molecules are able to block the active areas, resulting in deactivation of the fiber

Table 1. Constituents of oil of *Satureja hortensis* L

Compounds	RI[a]	HD[b] Area%	SPME[c] Area%	RSD[d]
Thujene	930	0.30	0.23	5.6
α-Pinene	936	6.34	5.14	8.2
α- Fenchene	950	0.06	0.02	4.5
Camphene	952	0.07	0.05	9.2
Verbenene	963	0.09	0.11	7.3
Heptanol-n	966	0.07	0.02	4.5
Trans-pinene	974	0.05	0.04	7.6
Sabinene	977	0.73	0.52	6.3
β- Pinene	981	0.06	0.03	9.1
Myrcene	992	1.23	0.92	8.5
α- Phellandrene	1005	31.65	24.21	7.6
ortho- Cymene	1021	8.34	5.33	5.1
β- Phellanderne	1029	5.72	5.12	4.6
Z-beta- Ocimene	1037	29.60	26.28	8.3
γ- Terpinene	1058	0.33	0.18	5.3
Terpinolene	1088	0.36	0.27	7.5
Linalool	1098	1.65	0.67	4.1
Cis-Thujone	1100	0.49	0.51	5.6
Allo-ocimene	1127	0.18	0.08	9.5
Cis-beta-terpineol	1142	0.20	0.18	9.2
Terpin-4-ol	1176	0.15	0.12	6.8
Cis-sabinene hydrate acetate	1219	0.84	0.28	8.5
Carvone	1239	3.03	2.06	9.2
Geraniol	1252	0.31	0.25	7.3
Thymol	1290	4.28	3.81	5.5
Carvacrol	1298	1.41	0.84	6.4
Z-jasmone	1392	0.21	0.07	8.3
Phenyl-hexan-3-one	1421	0.45	0.47	6.5
Germacrene D	1480	0.26	0.25	7.5
Cadina-1,4-diene	1532	0.12	0.08	8.2
Caryophylene alcohol	1568	0.07	0.03	5.4
Spathulenol	1576	1.02	0.89	7.6

[a] Retention indices using a HP-5 MS column.
[b] Relative area (peak area relative to total peak area) for hydrodistillation method.
[c] Relative area (peak area relative to total peak area except for the solvent peak) for SPME method.
[d] RSD values for SPME method (relative peak area).

surface. Hence, the fiber proposed here can serve as an optimal adsorptive fiber for sampling from dried materials.

MOF-HS-SPME of Satureja hortensis

The optimized MOF-HS-SPME conditions were applied to the extraction and concentration of the volatile constituents in *Satureja hortensis* with this fiber. The volatile compounds of *Satureja hortensis* were extracted and concentrated by MOF-HS-SPME (Fig. 4), and then the analytes that were exracted on fiber was desorbed and analyzed by GC–MS. The components were identified, and listed in Table 1. To investigate the reproducibility (fiber-to-fiber) and repeatability (for one fiber), five fibers were made in our work under the same circumstances and five repeated tests were performed utilizing each fiber. Table 1 represents the determined R.S.Ds.

Based on these data, good repeatability is found for the method. The relatively high fiber-to-fiber R.S.D. (≤9 %) shows that the coating volume probably differs considerably between fibers. Hence, improving the coating process is essential to ensure uniform and reproducible thickness. However, the made SPME fiber is mechanically

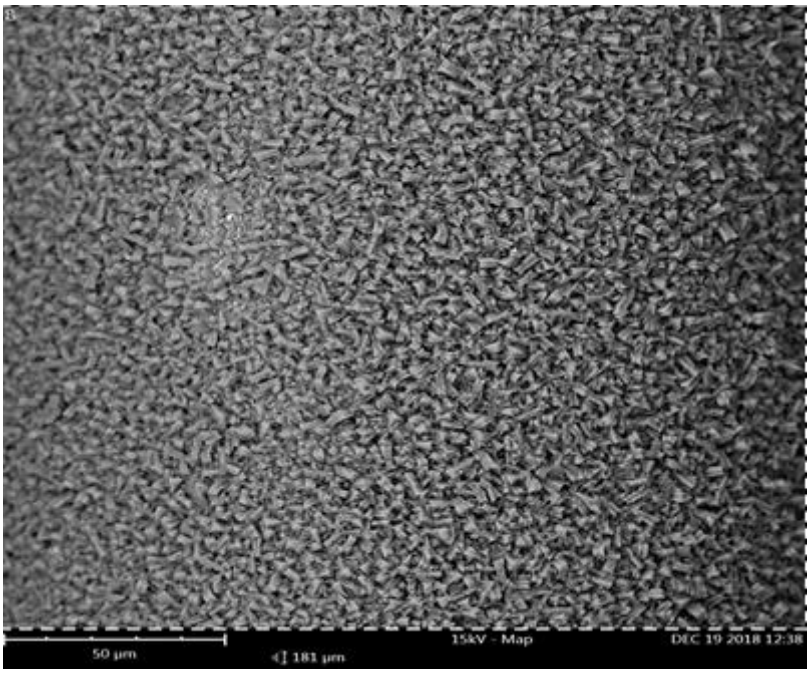

Fig.5. SEM image of Metal-organic framework on copper nanoarrays nanocomposite

stable and it does not require to utilize various fibers in the analysis. The SEM shows the structure and morphology in Fig. 5.

CONCLUSION

The present paper investigated the MOF wire efficiency as fiber for solid-phase microextraction of volatile substances in a medicinal herb. The suggested approach helped identification of 31 substances from *Satureja hortensis*. MOF-HS-SPME/GC–MS provides an efficient, quick, simple, and solvent-free approach for analyzing essential oils of *Satureja hortensis* as well as other herbs with a small sample amount compared to ordinary HD approach. The approach proposed here is an environment-friendly approach as it does not use any toxic solvent. Hence, no solvent peak is present in the chromatogram. The proposed fiber provides such advantages as inexpensiveness, high-temperature resistance, long durability, and hardness. This fiber was utilized here for the first time for analyzing volatile substances in medicinal herbs.

CONFLICT OF INTERESTS

The authors declare no conflict of interests.

REFERENCES

1. Čihák A. Biological Effects of 5-Azacytidine in Eukaryotes. Oncology. 1974;30(5):405-22. 10.1159/000224981
2. Kaminskas E, Farrell AT, Wang Y-C, Sridhara R, Pazdur R. FDA Drug Approval Summary: Azacitidine (5-azacytidine, Vidaza™) for Injectable Suspension. The Oncologist. 2005;10(3):176-82. 10.1634/theoncologist.10-3-176
3. Dapp Michael J, Clouser Christine L, Patterson S, Mansky Louis M. 5-Azacytidine Can Induce Lethal Mutagenesis in Human Immunodeficiency Virus Type 1. Journal of Virology. 2009;83(22):11950-8. 10.1128/JVI.01406-09
4. Diamantopoulos PT, Michael M, Benopoulou O, Bazanis E, Tzeletas G, Meletis J, et al. Antiretroviral activity of 5-azacytidine during treatment of a HTLV-1 positive myelodysplastic syndrome with autoimmune manifestations. Virology Journal. 2012;9(1):1. 10.1186/1743-422X-9-1
5. Stresemann C, Lyko F. Modes of action of the DNA methyltransferase inhibitors azacytidine and decitabine. International Journal of Cancer. 2008;123(1):8-13. https://doi.org/10.1002/ijc.23607
6. Navada SC, Steinmann J, Lübbert M, Silverman LR. Clinical development of demethylating agents in hematology. The Journal of Clinical Investigation. 2014;124(1):40-6. 10.1172/JCI69739
7. Subbanna S, Nagre NN, Shivakumar M, Basavarajappa BS. A single day of 5-azacytidine exposure during development induces neurodegeneration in neonatal mice and neurobehavioral deficits in adult mice. Physiology & Behavior. 2016;167:16-27. https://doi.org/10.1016/j.physbeh.2016.08.036
8. Salmani MM, Hashemian M, Yekta HJ, Nejad MG, Saber-Samandari S, Khandan A. Synergic Effects of Magnetic Nanoparticles on Hyperthermia-Based Therapy and

Controlled Drug Delivery for Bone Substitute Application. Journal of Superconductivity and Novel Magnetism. 2020;33(9):2809-20. 10.1007/s10948-020-05530-1
9. Sahmani S, Khandan A, Saber-Samandari S, Mohammadi Aghdam M. Effect of magnetite nanoparticles on the biological and mechanical properties of hydroxyapatite porous scaffolds coated with ibuprofen drug. Materials Science and Engineering: C. 2020;111:110835. https://doi.org/10.1016/j.msec.2020.110835
10. Kordjamshidi A, Saber-Samandari S, Ghadiri Nejad M, Khandan A. Preparation of novel porous calcium silicate scaffold loaded by celecoxib drug using freeze drying technique: Fabrication, characterization and simulation. Ceramics International. 2019;45(11):14126-35. https://doi.org/10.1016/j.ceramint.2019.04.113
11. Bakry R, Vallant RM, Najam-ul-Haq M, Rainer M, Szabo Z, Huck CW, et al. Medicinal applications of fullerenes. International journal of nanomedicine. 2007;2(4):639.
12. Kazemzadeh H, Mozafari M. Fullerene-based delivery systems. Drug Discovery Today. 2019;24(3):898-905. https://doi.org/10.1016/j.drudis.2019.01.013
13. Raza K, Thotakura N, Kumar P, Joshi M, Bhushan S, Bhatia A, et al. C60-fullerenes for delivery of docetaxel to breast cancer cells: A promising approach for enhanced efficacy and better pharmacokinetic profile. International Journal of Pharmaceutics. 2015;495(1):551-9. https://doi.org/10.1016/j.ijpharm.2015.09.016
14. Tagmatarchis N, Shinohara H. Fullerenes in medicinal chemistry and their biological applications. Mini Rev Med Chem. 2001;1(4):339-48. 10.2174/1389557013406684
15. Ye L, Kollie L, Liu X, Guo W, Ying X, Zhu J, et al. Antitumor Activity and Potential Mechanism of Novel Fullerene Derivative Nanoparticles. Molecules [Internet]. 2021; 26(11). 10.3390/molecules26113252
16. Kang S-H, Kim G, Kwon Y-K. Adsorption properties of chalcogen atoms on a golden buckyball Au16− from first principles. Journal of Physics: Condensed Matter. 2011;23(50):505301. 10.1088/0953-8984/23/50/505301
17. Mallawaarachchi S, Premaratne M, Maini PK. Superradiant Cancer Hyperthermia Using a Buckyball Assembly of Quantum Dot Emitters. IEEE Journal of Selected Topics in Quantum Electronics. 2019;25(2):1-8. 10.1109/JSTQE.2018.2867417
18. Kalaugher L. Buckyball pioneer dies. Physics World. 2005;18(12):9. 10.1088/2058-7058/18/12/11
19. Wang S, Poon K, Cai Z. Removal and metabolism of triclosan by three different microalgal species in aquatic environment. Journal of Hazardous Materials. 2018;342:643-50. https://doi.org/10.1016/j.jhazmat.2017.09.004
20. Adolfsson-Erici M, Pettersson M, Parkkonen J, Sturve J. Triclosan, a commonly used bactericide found in human milk and in the aquatic environment in Sweden. Chemosphere. 2002;46(9):1485-9. https://doi.org/10.1016/S0045-6535(01)00255-7
21. Zhao M, Huang Z, Wang S, Zhang L, Wang C. Experimental and DFT study on the selective adsorption mechanism of Au(◦) using amidinothiourea-functionalized UiO-66-NH2. Microporous and Mesoporous Materials. 2020;294:109905. https://doi.org/10.1016/j.micromeso.2019.109905
22. Khataee H, Ibrahim MY, Sourchi S, Eskandari L, Noranis MT. Computing optimal electronic and mathematical properties of Buckyball nanoparticle using graph algorithms. COMPEL-The international journal for computation and mathematics in electrical and electronic engineering. 2012;31(2):387-400.
23. Yavuz AE, Haman Bayarı S, Kazancı N. Structural and vibrational study of maprotiline. Journal of Molecular Structure. 2009;924-926:313-21. https://doi.org/10.1016/j.molstruc.2008.11.029
24. Garelli MS, Kusmartsev FV. Buckyball quantum computer: realization of a quantum gate. The European Physical Journal B - Condensed Matter and Complex Systems. 2005;48(2):199-206. 10.1140/epjb/e2005-00397-6
25. Trinh LH, Takzare A, Ghafoor DD, Siddiqi AF, Ravali S, Shalbaf M, et al. Trachyspermum copticum essential oil incorporated niosome for cancer treatment. Journal of Drug Delivery Science and Technology. 2019;52:818-24. https://doi.org/10.1016/j.jddst.2019.05.046
26. Ceulemans A, Muya JT, Gopakumar G, Nguyen MT. Chemical bonding in the boron buckyball. Chemical Physics Letters. 2008;461(4):226-8. https://doi.org/10.1016/j.cplett.2008.07.020
27. Muya JT, Nguyen MT, Ceulemans A. Quantum chemistry study of symmetric methyne substitution patterns in the boron buckyball. Chemical Physics Letters. 2009;483(1):101-6. https://doi.org/10.1016/j.cplett.2009.10.014
28. Jo S, Kim S, Lee BH, Tandon A, Kim B, Park SH, et al. Fabrication and Characterization of Finite-Size DNA 2D Ring and 3D Buckyball Structures. International Journal of Molecular Sciences [Internet]. 2018; 19(7). 10.3390/ijms19071895
29. Wang C, Huang W, Lin J, Fang F, Wang X, Wang H. Triclosan-induced liver and brain injury in zebrafish (Danio rerio) via abnormal expression of miR-125 regulated by PKCα/Nrf2/p53 signaling pathways. Chemosphere. 2020;241:125086. https://doi.org/10.1016/j.chemosphere.2019.125086
30. Kang T, Guan R, Chen X, Song Y, Jiang H, Zhao J. In vitro toxicity of different-sized ZnO nanoparticles in Caco-2 cells. Nanoscale Research Letters. 2013;8(1):496. 10.1186/1556-276X-8-496
31. Shirai Y, Osgood AJ, Zhao Y, Kelly KF, Tour JM. Directional Control in Thermally Driven Single-Molecule Nanocars. Nano Letters. 2005;5(11):2330-4. 10.1021/nl051915k
32. NazarAli Z, Ahmadi SA, Ghazanfari D, Sheikhhosseini E. Adsorption of Bupropion on C60 Nanocage: Thermodynamic and Electronic Properties. Nanochemistry Research. 2022;7(1):22-7.
33. Tavakoli S, Ahmadi SA, Ghazanfari D, Sheikhhosseini E. Theoretical investigation of functionalized fullerene nano carrier drug delivery of fluoxetine. Journal of the Indian Chemical Society. 2022;99(7):100561. https://doi.org/10.1016/j.jics.2022.100561
34. Najibzade Y, Sheikhhosseini E, Akhgar MR, Ahmadi SA. Absorption of tranylcypramine on C60 nanocage: Thermodynamic and electronic properties. Pakistan Journal of Pharmaceutical Sciences. 2022;35(3).
35. Razavi R, Kaya S, Zahedifar M, Ahmadi SA. Simulation and surface topology of activity of pyrazoloquinoline derivatives as corrosion inhibitor on the copper surfaces. Scientific Reports. 2021;11(1):12223. 10.1038/s41598-021-91159-6
36. Frisch M, Trucks G, Schlegel H, Scuseria G, Robb M, Cheeseman J, et al. Gaussian09, Rev. C. 01; Gaussian. Inc: Wallingford, CT. 2010.
37. Lee C, Wei X, Kysar JW, Hone J. Measurement of the Elastic Properties and Intrinsic Strength of Monolayer Graphene. Science. 2008;321(5887):385-8. 10.1126/science.1157996